Agricultural Water Management 118 (2013) 79–86

Contents lists available at SciVerse ScienceDirect

Agricultural Water Management

journal homepage: www.elsevier.com/locate/agwat

An insight to the performance of crop water stress index for olive trees

N. Agam[a,*], Y. Cohen[b], J.A.J. Berni[c], V. Alchanatis[b], D. Kool[a,d], A. Dag[a], U. Yermiyahu[a], A. Ben-Gal[a]

[a] Gilat Research Center, Agricultural Research Organization, Rural delivery Negev, 85280, Israel
[b] Institute of Agricultural Engineering, Agricultural Research Organization, Volcani Center, P.O. Box 6, Bet Dagan, 50250, Israel
[c] CSIRO Marine and Atmospheric Research, Black Mountain, 2601, ACT, Australia
[d] French Associates Institute for Agriculture and Biotechnology of Drylands, Blaustein Institutes for Desert Research, Ben-Gurion University of the Negev, Sede-Boker campus, 84990, Israel

ARTICLE INFO

Article history:
Received 11 May 2012
Accepted 3 December 2012

Keywords:
Canopy temperature
Crop water stress index
Fully transpiring leaf
Non-transpiring leaf
Olive tree
Water status

ABSTRACT

Optimization of olive oil quantity and quality requires finely tuned water management, as increased irrigation, up to a certain level, results in increasing yield, but a certain degree of stress improves oil quality. Monitoring tools that provide accurate information regarding orchard water status would therefore be beneficial. Amongst the various existing methods, those having high resolution, either temporally (i.e., continuous) or spatially, have the maximum adoption potential. One of the commonly used spatial methods is the Crop Water Stress Index (CWSI). The objective of this research was to test the ability of the CWSI to characterize water status dynamics of olive trees as they enter into and recover from stress, and on a diurnal scale. CWSI was tested in an empirical form and in two analytical configurations. In an experiment conducted in a lysimeter facility in the northwestern Negev, Israel, irrigation was withheld for 6 days for 5 of 15 trees, while daily irrigation continued for the rest of the trees. After resuming irrigation, the trees were monitored for 5 additional days. Water status measurements and thermal imaging were conducted daily between 12:00 and 14:00. Diurnal monitoring (predawn to after dusk) of the same indicators was conducted on the day of maximum stress. Continuous meteorological data were acquired throughout the experimental period. Empirical and analytical CWSI were calculated based on canopy temperature extracted from thermal images. The empirical CWSI differentiated between well watered and stressed trees, and depicted the water status dynamics during the drought and recovery periods as well as on a diurnal scale. Analytical approaches did not perform as well at either time scale. In conclusion, the empirical CWSI seems to be promising even given its limitations, while analytical forms of CWSI still require improvement before they can be used as a water status monitoring tool for olive orchards. Practically, it is proposed to compute the wet temperature analytically and set the dry temperature to 5 °C higher than air temperature.

1. Introduction

The importance of olive oil cannot be overemphasized. Recent widespread transition from traditional-rainfed to intensive-irrigated orchards, as well as profusion of new plantations, is well apparent in many Mediterranean areas and worldwide. It has also been indicated that optimization of olive oil quantity and quality requires finely tuned water management, as increased irrigation, up to a certain level, results in increasing yield, but a certain degree of stress improves oil quality (Ben-Gal et al., 2011a,b; Berenguer et al., 2006; Dag et al., 2008). Monitoring tools that provide accurate information regarding orchard water status would therefore be beneficial. Amongst the various existing methods, those having high resolution, either temporally (i.e., continuous) or spatially, while covering sufficient representative area, have the highest adoption potential (Ben-Gal et al., 2010).

Canopy temperature (T_C) has long been recognized as an indicator of plant water availability (Gates, 1964). Recent technological advances in remote thermal imaging offer the potential to acquire spatial information on surface temperature, and thus facilitate mapping of T_C variability over large areas. Mapping can be practiced at various scales from local (e.g., mounting an infrared thermometer on an elevated device) to regional (satellite images covering large areas, but at the expense of lower spatial resolution).

T_C is determined not only by the water status of the plant, but also by environmental conditions, primarily incoming short wave radiation, wind speed, air temperature and humidity. In order to use T_C as a water status indicator it must be normalized to account for the varying environmental conditions. One of the commonly used normalization methods is a temperature-based crop water stress

* Corresponding author. Tel.: +972 52 2292131; fax: +972 8 9926485.
E-mail addresses: agam@agri.gov.il, nurit.agam@gmail.com (N. Agam).

0378-3774/$ – see front matter © 2012 Elsevier B.V. All rights reserved.
http://dx.doi.org/10.1016/j.agwat.2012.12.004

index (CWSI) developed by Idso et al. (1981). The CWSI is a measure of relative transpiration (Jackson et al., 1981) and is defined as (Idso et al., 1981; Jackson et al., 1981):

$$\mathrm{CWSI} = \frac{T_C - T_{\mathrm{wet}}}{T_{\mathrm{dry}} - T_{\mathrm{wet}}} \quad (1)$$

in which T_{wet} is the temperature of a leaf transpiring at the maximum potential rate and T_{dry} is the temperature of a non-transpiring leaf. According to this definition, when a canopy is transpiring at its potential rate, $T_C = T_{\mathrm{wet}}$ and CWSI = 0. When the canopy is not transpiring, $T_C = T_{\mathrm{dry}}$ and CWSI = 1. This normalization is simple and reasonable, provided that T_{dry} and T_{wet} are known. Several theoretical formulations have been proposed to determine the CWSI, all based on energy balance equations.

The use of theoretical equations of CWSI based on the energy balance equation (Jackson et al., 1988) is limited by the need to estimate net radiation and aerodynamic resistance, but allows the calculation of canopy conductance (Leinonen et al., 2006; Lhomme and Monteny, 2000; Smith et al., 1988). Two analytical forms are discussed here, the first proposed by Jones ($\mathrm{CWSI_J}$; Jones, 1992, 1999) and the second by Berni et al. (2009) ($\mathrm{CWSI_B}$). The detailed formulations of both are found in the given references. Here, only the final forms, relevant to the discussion, are presented.

Jones (1992, 1999) determined the dry and wet temperatures required in Eq. (1) by solving for the surface energy balance. T_{dry}, the upper limit set as a non-transpiring leaf temperature, is computed assuming no transpiration flux, and T_{wet}, the lower limit set as a leaf transpiring at the potential rate, is computed assuming canopy resistance is negligible. This yields:

$$T_{\mathrm{dry}} = T_a + \frac{R_n r_{\mathrm{HR}}}{\rho C_P} \quad (2)$$

and

$$T_{\mathrm{wet}} = T_a - \frac{r_{\mathrm{HR}} r_V \gamma}{\rho C_P(\Delta r_{\mathrm{HR}} + \gamma r_V)} R_n + \frac{r_{\mathrm{HR}}}{\Delta r_{\mathrm{HR}} + \gamma r_V}\mathrm{VPD} \quad (3)$$

where T_a is air temperature; R_n is net radiation; r_{HR} is the combined resistance to sensible heat transport; ρ is dry air density; C_P is the specific heat of dry air at constant pressure; r_V is aerodynamic resistance to latent heat transport; γ the psychrometric constant; Δ is the slope of saturated water vapor pressure versus temperature curve; and VPD is vapor pressure deficit. See (Ben-Gal et al., 2009) for details on specific parameterizations.

In the approach of Berni et al. (2009), first the canopy resistance (r_c) is computed by:

$$r_c = \frac{r_a VPD}{\gamma((r_a R_n/\rho C_P) - (T_c - T_a))} \quad (4)$$

in which r_a is the aerodynamic resistance. Once r_c is known, and the potential canopy resistance for a well watered crop (r_{cp}) is estimated (see Moriana and Fereres, 2002; and Testi et al., 2006 for olive trees), an analytical solution for the CWSI may be obtained (Jackson et al., 1981):

$$\mathrm{CWSI_B} = \frac{\gamma(r_c - r_{\mathrm{cp}}/r_a)}{\Delta + \gamma(1 + (r_{\mathrm{cp}}/r_a))} \quad (5)$$

When $r_c = r_{\mathrm{cp}}$, i.e., water vapor conduction through the stomata is at its potential rate, $\mathrm{CWSI_B} = 0$. When the stomata are closed and $r_c \to \infty$, $\mathrm{CWSI_B} \to 1$. By defining a value for r_{cp} rather than setting canopy resistance of well watered plants to zero, a more realistic description of the system is achieved.

Additional recent studies proposed the use of empirical dry and wet reference temperatures, allowing the estimation of CWSI with a minimum of meteorological measurements (Cohen et al., 2005; Grant et al., 2007; Jones et al., 2002; Moller et al., 2007). In such an empirical approach ($\mathrm{CWSI_E}$), T_{dry} is set to 5 °C greater than air temperature (Jackson, 1982) and T_{wet} is determined based on measurements of a wet artificial reference surface (WARS) captured by the thermal image. This approach can only be applied to measurements at a local scale, i.e., when proximal thermal images are taken.

Two main drawbacks limit the applicability of $\mathrm{CWSI_E}$ for high spatiotemporal monitoring of stress (Ben-Gal et al., 2009). The first is the empirical value of 5 °C. While it had indeed been proven to represent the maximum leaf temperature under several conditions (Cohen et al., 2005; Irmak et al., 2000; Moller et al., 2007), the $\mathrm{CWSI_E}$ is quite sensitive to the value assigned to T_{dry}, and a significant uncertainty is induced to the index's value when use of this empirical formulation is adopted. The second drawback lies in the need for a wet reference to exist in every analyzed image. This restricts the frequency in which data can be acquired, thus limiting the usefulness of the method for routine measurements.

The analytical formulations potentially overcome the mentioned setbacks of the empirical approach, provided they yield accurate and reliable results. Ben-Gal et al. (2009) tested both the analytical and the empirical methods in an olive orchard with irrigation treatments, and found both methods to perform well, with no statistically significant difference between them. Their conclusions were based on a single day of measurement. However, when the aim is to provide a management tool that will assure specific water status conditions, the technique should be able to not only separate between water status levels, but also follow water status dynamics. The objective of this research was to test the ability of the CWSI to detect dynamics in canopy temperatures reflecting relative transpiration of trees under different water status conditions. The CWSI was tested, in its empirical form as well as in two analytical forms, both on a diurnal and a day-to-day timescale by monitoring individual trees via proximal thermal imagery as they entered into and recovered from stress.

2. Materials and methods

2.1. Experimental setup

Single 2-year-old 'Barnea' olive trees were planted in fifteen 2.5 $\mathrm{m^3}$ volume free-standing lysimeters at the Gilat Research Center in the northwestern Negev, Israel (31°20′N, 34°40′E) in June 2008. Full details on the experimental setup are given by Ben-Gal et al. (2010). Tree volume, estimated by multiplying the tree upper transect, calculated from RGB images, by measured tree height, was $31.3 \pm 7.3\ \mathrm{m^3}$. The row spacing between the trees was 2.5 m and within row distance was 4 m.

The lysimeters' weights were continuously monitored, and their soil surface covered by a water permeable geotextile (Non-Woven Geotextile, 500 $\mathrm{g\,m^{-2}}$, Noam-Urim, Israel). Since the soil surface was completely shaded both by the geotextile mulch and by the tree canopies themselves, evaporation losses were assumed to be negligible. Thus, transpiration rates (T) of individual trees were computed by

$$T = I - D - \Delta W \quad (6)$$

where I is irrigation, D is drainage, and ΔW is mass change representing change in soil water content.

Prior to the initiation of the experiment, the trees were irrigated daily with quantities always exceeding previous days' transpiration rates.

Starting in August 28, 2009 irrigation was withheld for 5 of the 15 trees, and by September 2 they were transpiring ~10% of the well watered trees and were severely stressed (Ben-Gal et al., 2010). On September 3, irrigation was resumed. Daily irrigation continued for the rest of the trees at all times. Hereafter, August 28–September 2

will be referred to as the "drought period", and September 3–7, during which all physiological parameters returned to their reference values or stabilized on new values, will be termed the "recovery period". See Ben-Gal et al. (2010) for more details on the experimental setup and physiological monitoring.

Continuous meteorological data were acquired from a weather station 200 m from the site and actual transpiration rates were computed from the lysimeter water balance. During the drought and recovery periods, water status measurements were conducted daily between 12:00 and 14:00 local standard time on all trees. These included canopy temperature (see details below) and stomatal conductance from a diffusion leaf porometer (SC-1, Decagon Devices, Inc., Pullman, WA, USA) measured on five leaves fully exposed to sunlight on each tree. The daily monitoring continued after re-watering until full recovery was observed.

In order to capture the diurnal behavior of the different parameters on both well-irrigated and drought-stressed trees, the measurements were augmented and conducted throughout the day on September 2, the day before re-watering (day of minimum available water, minimum ET and maximum water stress). Diurnal monitoring started predawn (4:00) and continued until after dusk (20:00).

2.2. Thermal images acquisition and analysis

Thermal images were acquired using an un-cooled infrared thermal camera (ThermaCAM model SC2000, FLIR Systems Inc., USA) and ThermaCam researcher professional software (FLIR Systems Inc., USA). The camera has a 320 × 240 pixels microbolometer sensor, sensitive to the 7.5–13 μm spectral range, and a lens with an angular field of view of 24°. For accurate temperature extraction emissivity, air temperature and relative humidity were entered. Leaf emissivity was set to 0.98 and meteorological conditions values were entered from the meteorological station. The camera was mounted on a crane about 3 m above the canopy, yielding a resolution of 0.3 cm. Each image captured a single tree canopy and a WARS which its temperature was used as T_{wet} in $CWSI_E$ (see Fig. 1 for an example of stressed and well watered trees). Thermal images of two well watered and two stressed trees were captured at every measurement point. The WARS was constructed from a 5 cm thick slab of expanded polystyrene foam that floated in a 40 cm × 30 cm × 12 cm tray, covering most of the water surface. The slab was coated with a water absorbent non-woven polyester and viscose mixture cloth (Spuntech, Israel), overlaid on polyester non-woven water-absorbent cloth. The edges of the cloth served as a wick, soaking up water to replace evaporation, and the polystyrene foam insulated the float from the background (Meron et al., 2003; Moller et al., 2007). The WARS formed a permanently wet surface of reproducible radiometric and physical properties. Tree canopy temperatures (T_C) were determined by averaging pixels extracted from the central area of the canopy (ThermaCam researcher professional software). Similarly, polygons in the WARS in each image were delineated to extract its temperature. $CWSI_E$, $CWSI_J$ and $CWSI_B$ were computed for each image using Eq. (1). While T_C was identical for each of the three indices they were different in their reference values. For $CWSI_E$ T_{dry} was set to T_{air} + 5 °C and T_{wet} was set as the WARS temperature. For $CWSI_J$ T_{wet} and T_{dry} were computed using Eqs. (2) and (3), respectively and for the calculation of $CWSI_B$ Eqs. (4) and (5) were used.

2.3. Meteorological conditions throughout the experiment

The main meteorological conditions throughout the experiment are presented in Fig. 2. Incoming shortwave radiation (panel a) indicates partly cloudy sky to varying extent every day except for August 29. Until September 4, the sky cleared each day around noon

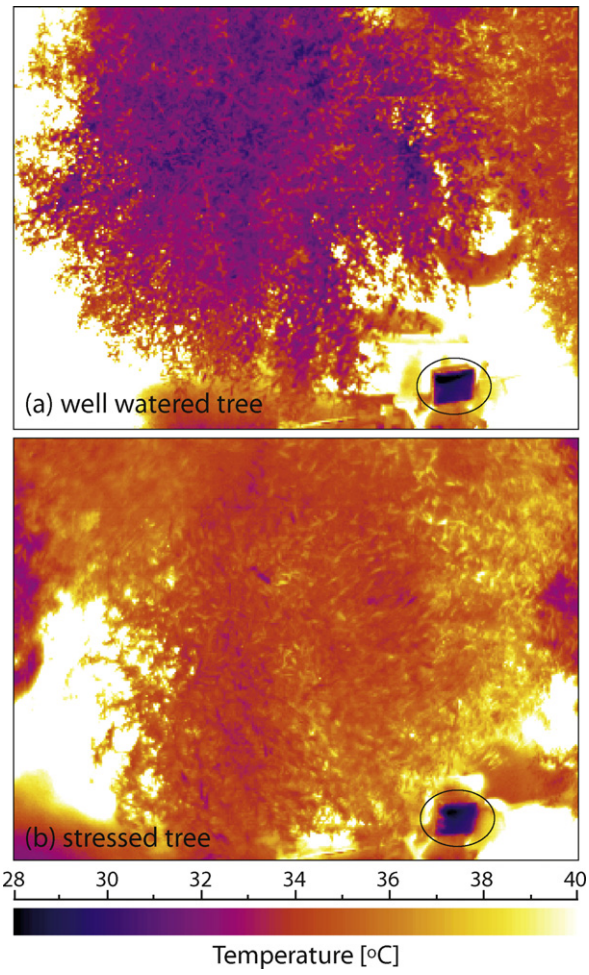

Fig. 1. Example of thermal images of (a) a well watered tree and (b) a stressed tree, taken at 1300 on September 2, 2009 (day of maximum stress). The ellipsoids mark the wet artificial reference surface.

(12:00). On September 2, except for a short period in the morning (~9:00–11:00), the sky was clear. Roughly, there was very little variation in air temperature and wind speed patterns during the experiment, with some variation in the relative humidity during daytime, corresponding to variations in cloud conditions. In general, the days were warm (temperatures reaching maximums of above 30 °C every day), and the relative humidity fluctuated from 30 to 40% at noon to above 80% at night.

3. Results and discussion

3.1. Transpiration rates

Transpiration rates obtained from the lysimeters were used as the basis against which the performance of CWSI computations was tested, both along the drought and recovery periods and diurnally. Transpiration data is therefore presented (Fig. 3), in spite of being published previously (Ben-Gal et al., 2010), in order to show the water status dynamics of the stressed and well watered groups.

Transpiration rates of all trees were similar prior to the cessation of irrigation to 5 of the trees, with totals of about 80 L per tree per day (Fig. 3a). The well watered group maintained a more or less constant level of transpiration throughout the experiment, while a sharp reduction in transpiration was observed for the stressed trees. On September 2nd, one day before resumption of irrigation,

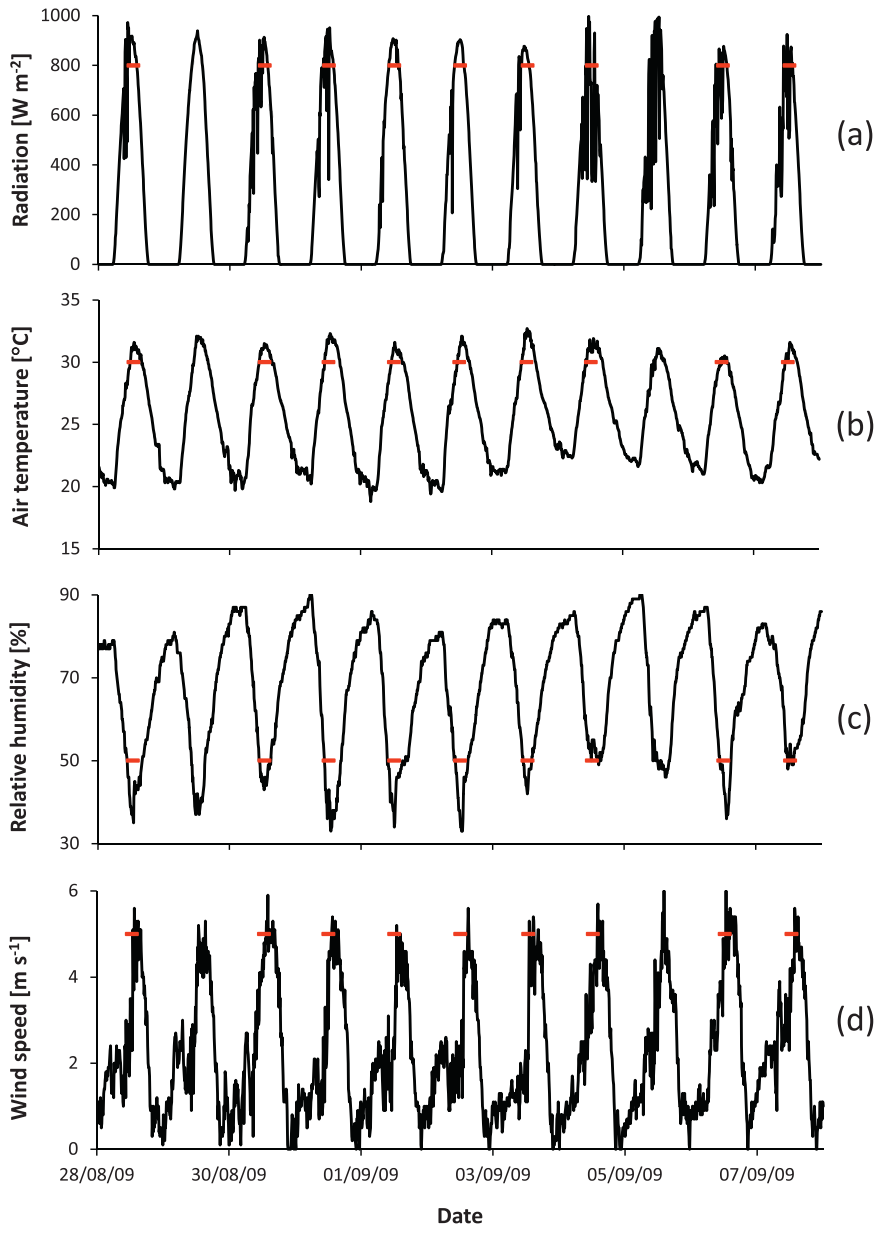

Fig. 2. Meteorological conditions throughout the experiment: (a) solar radiation; (b) air temperature; (c) relative humidity; and (d) wind speed. Red marks show the time at which measurements were conducted.

the trees were most stressed and transpired only ~15% of the initial amount. Once irrigation was resumed, transpiration increased, and by the 5th day (September 7) stabilized at ~85% of the initial amount, but did not reach 100% even after 2 weeks (see more details in Ben-Gal et al., 2010).

Maximum daily rates of transpiration were measured between 13:00 and 15:00 each day. Maximum rates for well watered trees were ~9–10 L h^{-1} $tree^{-1}$. Maximum rates of the trees (in l h^{-1} $tree^{-1}$), well watered or stressed, were closely proportional (around 12%) to their daily total values (l day^{-1} $tree^{-1}$). The diurnal pattern of transpiration on September 2nd (the day of maximum stress) was significantly different for the well watered and stressed trees (Fig. 3b). While the well watered trees showed continuously increasing rates of transpiration from the morning through 14:00 with a sharp decrease thereafter, the maximum transpiration rate of the stressed trees was at 10:00 in the morning.

3.2. Stress and recovery dynamics

Detection of stress and recovery dynamics by the three forms of CWSI was tested (Fig. 4) to examine the ability of the CWSI to monitor variations of increasing magnitude of water stress. CWSI was hypothesized to increase during stress and decrease during recovery, and to maintain a relatively stable value for the well watered trees. In the case of $CWSI_E$ (Fig. 4a), the well watered trees, as expected, maintained a relatively constant $CWSI_E$ value throughout the experiment (with a range of 0.18–0.37), while the $CWSI_E$ of the stressed trees increased as the trees went into stress and gradually decreased in the recovery period. This behavior mimicked the pattern of measured transpiration rates (Fig. 3a), further strengthening the potential use of $CWSI_E$ for water status monitoring of olive trees.

However, both analytically computed CWSI poorly followed the dynamics of water status (Fig. 4b and c for $CWSI_I$ and $CWSI_B$,

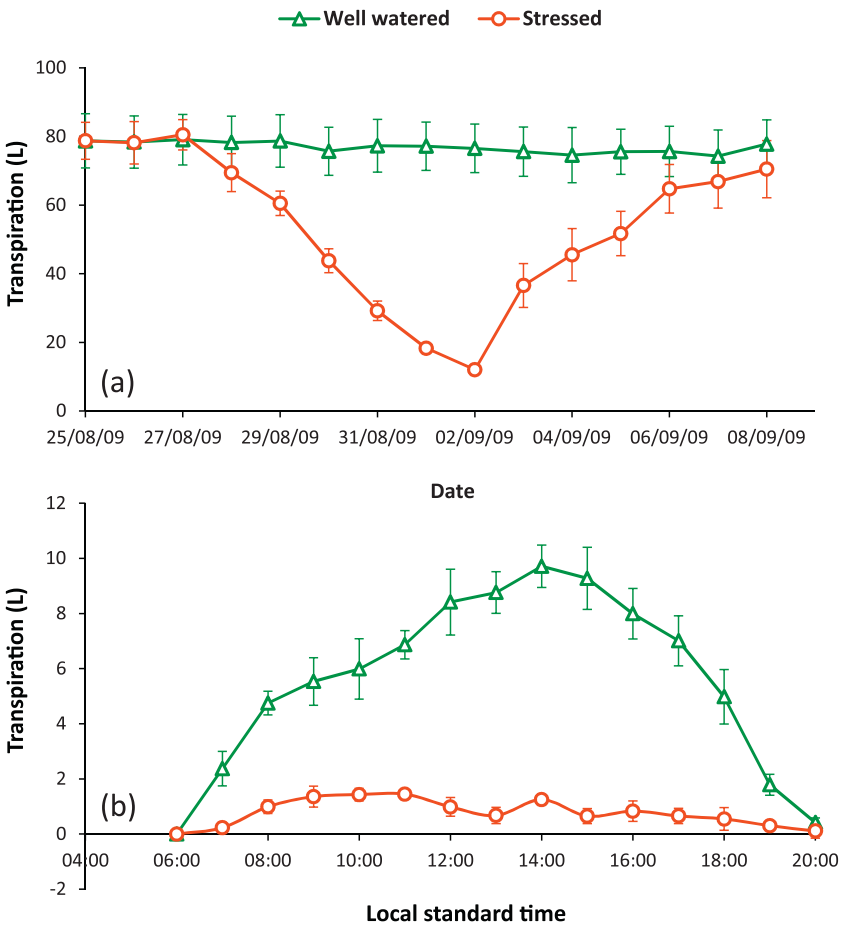

Fig. 3. Lysimeter measurements of transpiration of well watered and stressed trees. (a) Daily total transpiration; (b) diurnal transpiration measured on day of maximum stress (September 2, 2008). After Ben-Gal et al. (2010). Error bars show standard deviation.

respectively). In both, the well watered CWSI fluctuated throughout the experiment, much more pronouncedly than the empirical CWSI, while in theory they should have maintained a constant value near zero. The stressed CWSI also fluctuated throughout the experiment. While in both analytical forms the stressed trees' CWSI values were higher than those of the well watered trees, the dynamics of entering into and recovering from stress were less clear than for the case of the empirical form. The ranges of analytical CWSI values were also smaller than expected. Maximum and minimum values of $CWSI_J$ and $CWSI_B$ (Table 1) emphasize the low separability of stressed and well watered trees using these two methods. This makes their immediate use for olive orchards problematic. These results contradict the conclusions of Ben-Gal et al. (2009) who stated that: "*As both indices* [$CWSI_E$ and $CWSI_J$] *yielded similar results, and given the relative practicality of the analytical index, it appears that the analytical CWSI has an advantage over the empirical CWSI*". Nevertheless, while there seem to be issues with the absolute values of CWSI in both analytical methods, subtraction of CWSI of the stressed trees from well watered CWSI revealed the dynamic of entering into and recovering from stress (Fig. 5). From Fig. 5 it can also be seen that the maximum difference between stressed and well watered trees was smallest for $CWSI_J$ and similar for $CWSI_B$ and $CWSI_E$, indicating that $CWSI_J$ was the least able to separate between stressed and well watered trees.

Table 1
Minimum and maximum values of CWSI computed following Jones ($CWSI_J$; Jones, 1999) and Berni et al. ($CWSI_B$; Berni et al., 2009.)

	$CWSI_J$		$CWSI_B$	
	Well watered	Stressed	Well watered	Stressed
Minimum	0.67	0.78	0.13	0.36
Maximum	0.88	0.96	0.59	0.66

3.3. Diurnal dynamics of CWSI

The CWSI proposed by Jones (1999) was meant for detecting water status of plants around noon. If proven accurate during a longer period throughout the day, its application in practice will become more flexible. The ability of the CWSI to follow the diurnal course of water status was therefore examined. It was expected that CWSI of well watered trees would remain close to zero during any given measurement time, while CWSI of stressed trees would show a diurnal pattern representing the severity of the stress throughout the day. The transpiration rate of the well watered trees represents the potential transpiration, and its diurnal course was anticipated to follow the course of the evaporative demand. For the stressed trees, CWSI was expected to increase with increase in evaporative demand, and thus it was predicted that the diurnal course of the CWSI of stressed trees would be similar to the transpiration curve of the well watered trees (Fig. 3b). Indeed, the diurnal course of $CWSI_E$ (Fig. 6a) for the stressed and well watered trees followed the hypothesized patterns. The well watered trees maintained low and relatively constant levels of $CWSI_E$ while $CWSI_E$ of the stressed trees did increase until early afternoon and decreased thereafter, closely following the transpiration rates of the well watered trees.

A quite different pattern was obtained from the calculations of $CWSI_J$ and $CWSI_B$ (Fig. 6b and c, respectively). In both cases, a clear

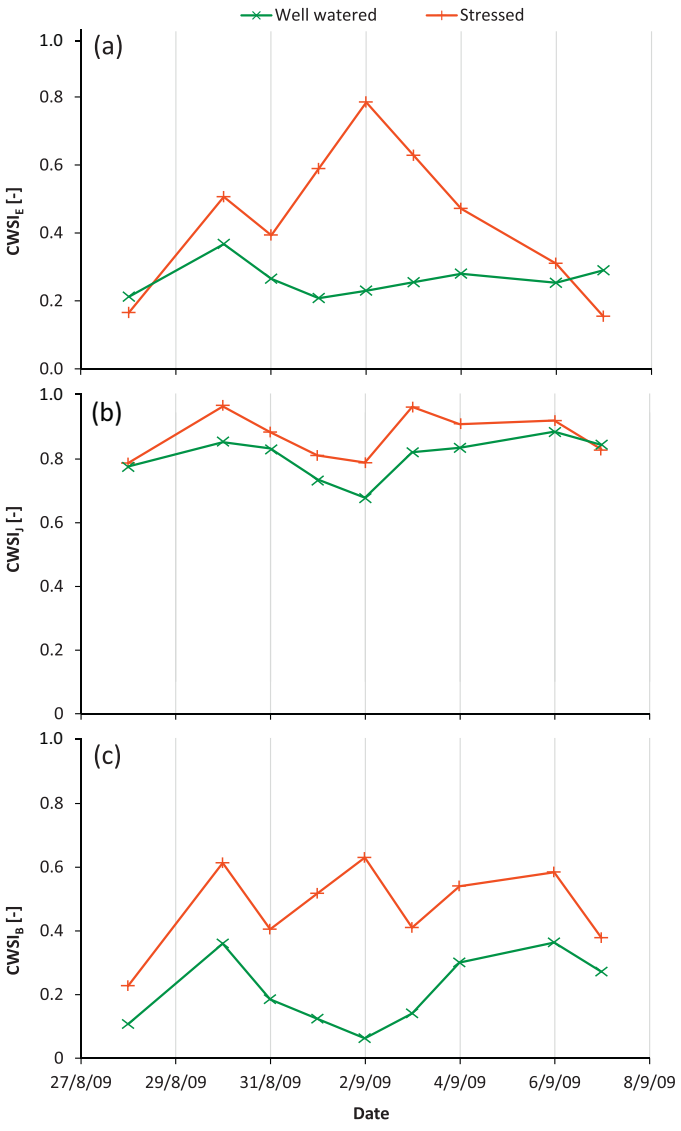

Fig. 4. Crop water stress index (CWSI) computed for noon-time (~12:00) measurements throughout the experiment. (a) Empirical CWSI; (b) analytical CWSI computed following Jones (1999); (c) analytical CWSI computed following Berni et al. (2009).

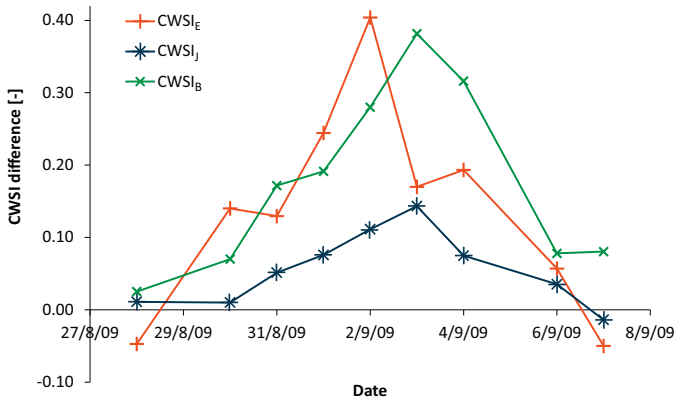

Fig. 5. Crop water stress index (CWSI) differences between well watered and stressed trees obtained by the three methods (CWSI$_E$, CWSI$_J$, and CWSI$_B$).

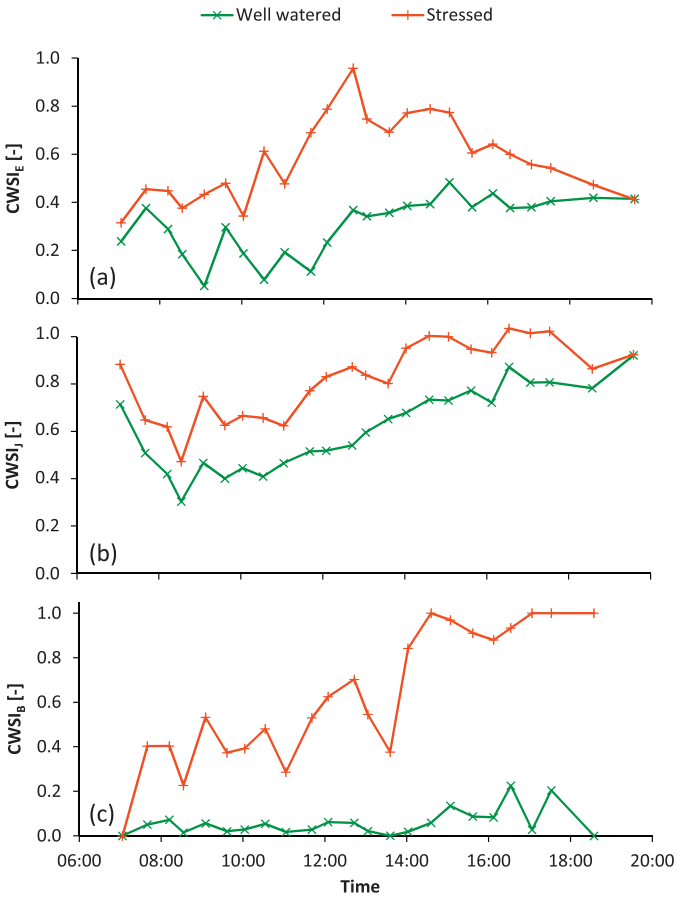

Fig. 6. Diurnal curves of crop water stress index (CWSI) for well watered and stressed trees as detected on the day of maximum stress by (a) empirical CWSI; (b) analytical CWSI computed following Jones (1999); (c) analytical CWSI computed following Berni et al. (2009).

difference was obtained between the well watered and the stressed groups. However, CWSI of the stressed trees showed a continuous increase throughout the day, with no decrease in the afternoon. This behavior does not have a physical explanation, and indicates that neither of these two indices is capable of following the diurnal dynamics of stress. Sections 3.3.1 and 3.3.2 discuss the reasoning for the misrepresentation of CWSI$_J$ and CWSI$_B$, respectively.

3.3.1. *CWSI$_J$*

To explore the reason for the diurnal behavior of CWSI$_J$, computations of the index were repeated, substituting first T_{wet} and then T_{dry} with the empirical values (Fig. 7a and b respectively). Substitution of T_{wet} increased the range of values as well as the difference between the stressed and well watered trees, but did not change the pattern of decreasing early in the morning and then increasing throughout the day. In contrast, substitution of T_{dry} resulted in a completely different, much more realistic, pattern of increase from the morning until early afternoon followed by a decrease.

This implies that something is incorrect in CWSI$_J$'s formulation or parameterization of T_{dry} (Eq. (2)). As explained above, T_{wet} simulates the temperature of a fully transpiring leaf and T_{dry} is formulated based on the assumption that a stressed leaf does not transpire at all. A well watered tree transpires at the potential rate depending on the evaporative demand, and is thus expected to follow the diurnal dynamics of the environmental conditions. A stressed tree is likely to slightly transpire during the early morning (Fig. 3b), a process that contradicts the assumption of no transpiration. Therefore, the estimated values of CWSI in this case will

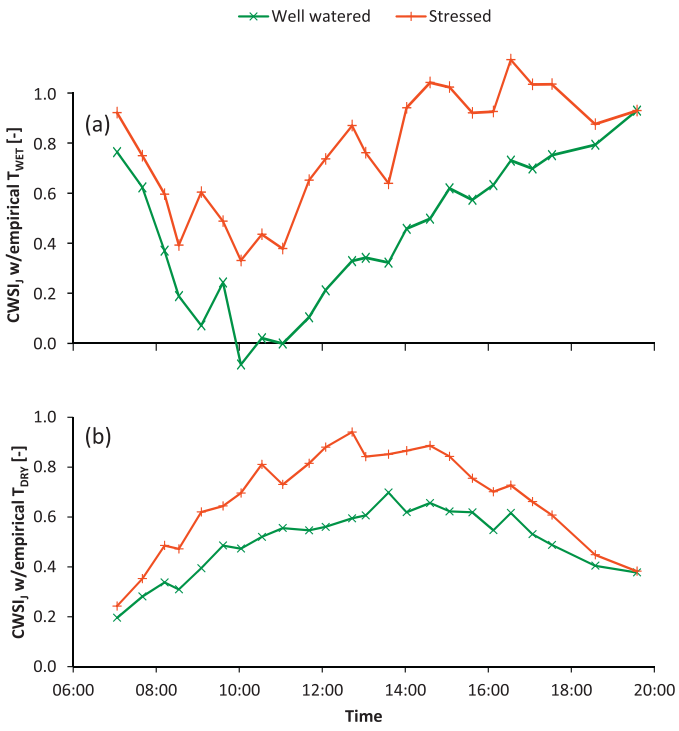

Fig. 7. Diurnal curves of crop water stress index computed following Jones (1999) ($CWSI_J$) with (a) T_{wet} substituted with T_{wet} empirical; and (b) T_{dry} substituted with T_{dry} empirical.

always be biased and underestimate the tree stress. Another potential source of error is a misrepresentation of one or more of the variables in the equation, namely air temperature (T_a), net radiation (R_n), or the aerodynamic resistance to sensible heat (r_{HR}). The measurement and computation of the first two is straight forward and well established and therefore it is most likely that the problem with the computation of $CWSI_J$ is in the way r_{HR} is parameterized to describe the aerodynamic resistance in olive trees. Although r_{HR} is also included in T_{wet}, its effect on the overall estimate of T_{wet} is weaker, thus it does not significantly alter the diurnal pattern. A deeper insight into the parameterization of r_{HR} for olive trees is required before a wide application of the method can be suggested. That said, it must be noted that the CWSI proposed by Jones (1999) was meant for detecting water status of plants around noon, a time during which the basic assumptions do hold, and trying to follow a diurnal course with this method may be untenable.

3.3.2. $CWSI_B$

In order to understand the diurnal behavior of $CWSI_B$, stomatal conductance (g_s, the reciprocal of stomatal resistance; Monteith and Unsworth, 2008), computed as the reciprocal of canopy resistance (Eq. (5)), was examined (Fig. 8). The computed g_s for the well watered trees showed a sharp increase in the morning, with a distinct peak soon after 8:00, and a gradual decrease thereafter, reaching complete stomatal closure at sunset. The stressed trees had a similar pattern with a significantly lower magnitude (peak value of the stressed trees was 1/3 of that of the well watered), and complete stomatal closure was reached at ~14:00. This pattern is similar to patterns observed for olives by e.g., Berni et al. (2009), Orgaz et al. (2007), Villalobos et al. (2000), and Fernandez et al. (1997). This indicates that the formulation of canopy conductance is realistic and yielded good results for both well watered and stressed cases. $CWSI_B$ of the well watered trees remained very low throughout the day (Fig. 6c). This is likely due to the way r_{cp} was determined. Since no empirical relationship was available from

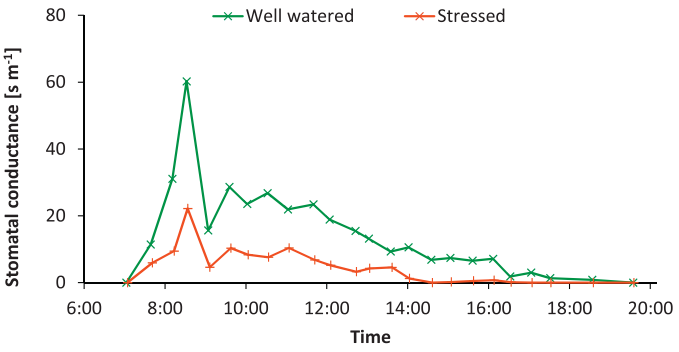

Fig. 8. Stomatal conductance of well watered and stressed trees computed following Berni et al. (2009).

prior measurements, and given the fact that the well watered trees received more than sufficient water for uptake and transpiration (by maintaining a daily amount of drainage), r_{cp} was taken as the minimum r_c at each given time step. However, $CWSI_B$ failed to detect the correct diurnal pattern for the stressed trees and continuously increased throughout the day, reaching a maximum toward late afternoon. This may be attributed to the fact that $CWSI_B$ is strongly dependent on calculated g_s (or r_c, see Eq. (5)). Since g_s decreases continuously throughout the day (Fig. 8) $CWSI_B$ corresponds with a continuous increase until late afternoon. It is likely that $CWSI_B$ is actually more an indirect estimate of stomatal conductance than it is an appraisal of tree water status.

3.4. A note on the limitation of the experimental setup

An important point to rise is that the olive trees in this experiment were grown in free standing lysimeters on top of weighing systems, such that the soil surface was ~1.5 m above the ground. While providing unique information on actual measured transpiration rates, which cannot be achieved otherwise, this setup may have an effect on the micro-meteorological characteristics of the "field" which was not accounted for in the computations.

4. Summary and conclusions

The objective of this research was to test the ability of the CWSI to detect water status dynamics both on a diurnal scale, and on a day-to-day timescale while monitoring olive trees as they entered into- and recovered from stress. CWSI was tested in its empirical form as well as in two analytical forms.

The empirical CWSI differentiated between the well watered and the stressed trees, and depicted the water status dynamics both during the drought and recovery periods and on a diurnal scale. In contrast, the analytical approaches ($CWSI_J$ and $CWSI_B$) failed to capture the dynamics on both time scales. In the case of $CWSI_J$ this is likely due to misrepresentation of the aerodynamic resistance to sensible heat transport in olive. The diurnal course of $CWSI_B$ was strongly affected by the diurnal course of canopy resistance, thus it may be considered more an indirect estimate of stomatal conductance than an indicator of tree water status.

The most pronounced applicative limitation of the $CWSI_E$ is the need for an artificial wet reference in each image, for obtaining T_{wet}. Considering that computed T_{wet} following Jones (1999) proved to yield good CWSI values, while T_{dry} was poorly estimated, it is therefore proposed to combine $CWSI_J$ with $CWSI_E$ to form a $CWSI_{JE}$. In $CWSI_{JE}$, T_{wet} is calculated analytically and T_{dry} is determined empirically (i.e., $T_{dry} = T_{air} + 5$). This necessitates meteorological measurements in or near by the field, while eliminating the need for a wet reference.

Acknowledgements

The building and maintaining of the lysimeter facility was supported generously by the JCA Charitable Foundation (ICA Israel). Thanks to Eugene Presnov of Gilat Research Center, Agricultural Research Organization of Israel, for technical assistance, to Asher Levi and Roman Brikman of the Institute of Agricultural Engineering, Agricultural Research Organization of Israel, for their crucial assistance in the acquisition of the thermal images, and to Alexander Goldberg of the Remote Sensing Laboratory, Blaustain Institutes for Desert Research, Ben-Gurion University of the Negev, for the analysis of the images.

References

Ben-Gal, A., Agam, N., Alchanatis, V., Cohen, Y., Yermiyahu, U., Zipori, I., Presnov, E., Sprintsin, M., Dag, A., 2009. Evaluating water stress in irrigated olives: correlation of soil water status, tree water status, and thermal imagery. Irrigation Science 27, 367–376.

Ben-Gal, A., Dag, A., Basheer, L., Yermiyahu, U., Zipori, I., Kerem, Z., 2011a. The influence of bearing cycles on olive oil quality response to irrigation. Journal of Agricultural and Food Chemistry 59, 11667–11675.

Ben-Gal, A., Kool, D., Agam, N., van Halsema, G.E., Yermiyahu, U., Yafe, A., Presnov, E., Erel, R., Majdop, A., Zipori, I., Segal, E., Ruger, S., Zimmermann, U., Cohen, Y., Alchanatis, V., Dag, A., 2010. Whole-tree water balance and indicators for short-term drought stress in non-bearing 'Barnea' olives. Agricultural Water Management 98, 124–133.

Ben-Gal, A., Yermiyahu, U., Zipori, I., Presnov, E., Hanoch, E., Dag, A., 2011b. The influence of bearing cycles on olive oil production response to irrigation. Irrigation Science 29, 253–263.

Berenguer, M.J., Vossen, P.M., Grattan, S.R., Connell, J.H., Polito, V.S., 2006. Tree irrigation levels for optimum chemical and sensory properties of olive oil. Horticultural Science 41, 427–432.

Berni, J.A.J., Zarco-Tejada, P.J., Sepulcre-Canto, G., Fereres, E., Villalobos, F., 2009. Mapping canopy conductance and CWSI in olive orchards using high resolution thermal remote sensing imagery. Remote Sensing of Environment 113, 2380–2388.

Cohen, Y., Alchanatis, V., Meron, M., Saranga, Y., Tsipris, J., 2005. Estimation of leaf water potential by thermal imagery and spatial analysis. Journal of Experimental Botany 56, 1843–1852.

Dag, A., Ben-Gal, A., Yermiyahu, U., Basheer, L., Nir, Y., Kerem, Z., 2008. The effect of irrigation level and harvest mechanization on virgin olive oil quality in a traditional rain-fed 'Souri' olive orchard converted to irrigation. Journal of the Science of Food and Agriculture 88, 1524–1528.

Fernandez, J.E., Moreno, F., Giron, I.F., Blazquez, O.M., 1997. Stomatal control of water use in olive tree leaves. Plant and Soil 190, 179–192.

Gates, D.M., 1964. Leaf temperature and transpiration. Agronomy Journal 56, 273–277.

Grant, O.M., Tronina, L., Jones, H.G., Chaves, M.M., 2007. Exploring thermal imaging variables for the detection of stress responses in grapevine under different irrigation regimes. Journal of Experimental Botany 58, 815–825.

Idso, S.B., Jackson, R.D., Pinter, P.J., Reginato, R.J., Hatfield, J.L., 1981. Normalizing the stress-degree-day parameter for environmental variability. Agricultural and Forest Meteorology 24, 45–55.

Irmak, S., Haman, D.Z., Bastug, R., 2000. Determination of crop water stress index for irrigation timing and yield estimation of corn. Agronomy Journal 92, 1221–1227.

Jackson, R.D., 1982. Canopy temperature and crop water stress. In: Hillel, D. (Ed.), Advances in Irrigation. Academic Press, New-York.

Jackson, R.D., Idso, S.B., Reginato, R.J., Pinter, P.J., 1981. Canopy temperature as a crop stress indicator. Water Resources Research 17, 1133–1138.

Jackson, R.D., Kustas, W.P., Choudhury, B.J., 1988. A reexamination of the crop water stress index. Irrigation Science 9, 309–317.

Jones, H.C., 1992. Plants and Microclimate. Cambridge University Press, Cambridge.

Jones, H.G., 1999. Use of infrared thermometry for estimation of stomatal conductance as a possible aid to irrigation scheduling. Agricultural and Forest Meteorologyis 95, 139–149.

Jones, S.B., Wraith, J.M., Or, D., 2002. Time domain reflectometry measurement principles and application. Hydrological Processes 16, 141–153.

Leinonen, I., Grant, O.M., Tagliavia, C.P.P., Chaves, M.M., Jones, H.G., 2006. Estimating stomatal conductance with thermal imagery. Plant, Cell & Environment 29, 1508–1518.

Lhomme, J.P., Monteny, B., 2000. Theoretical relationship between stomatal resistance and surface temperatures in sparse vegetation. Agricultural and Forest Meteorology 104, 119–131.

Meron, M., Tsipris, J., Charitt, D., 2003. Remote map of crop water status to assess spatial variability of crop stress. In: Strafford, J., Werner, A. (Eds.), Precision Agriculture. The fourth European Conference on Precision Agriculture. Academic Publishers, Berlin, pp. 405–410.

Moller, M., Alchanatis, V., Cohen, Y., Meron, M., Tsipris, J., Naor, A., Ostrovsky, V., Sprintsin, M., Cohen, S., 2007. Use of thermal and visible imagery for estimating crop water status of irrigated grapevine. Journal of Experimental Botany 58, 827–838.

Monteith, J.L., Unsworth, M.H., 2008. Principles of Environmental Physics, 3rd ed. Academic Press, Elsevier.

Moriana, A., Fereres, E., 2002. Plant indicators for scheduling irrigation of young olive trees. Irrigation Science 21, 83–90.

Orgaz, F., Villalobos, F.J., Testi, L., Fereres, E., 2007. A model of daily mean canopy conductance for calculating transpiration of olive canopies. Functional Plant Biology 34, 178–188.

Smith, R.C.G., Barrs, H.D., Fischer, R.A., 1988. Inferring stomatal resistance of sparse crops from infrared measurements of foliage temperature. Agricultural and Forest Meteorology 42, 183–198.

Testi, L., Orgaz, F., Villalobos, F.J., 2006. Variations in bulk canopy conductance of an irrigated olive (*Olea europaea* L.) orchard. Environmental and Experimental Botany 55, 15–28.

Villalobos, F.J., Orgaz, F., Testi, L., Fereres, E., 2000. Measurement and modeling of evapotranspiration of olive (*Olea europaea* L.) orchards. European Journal of Agronomy 13, 155–163.